

RESEARCH ARTICLE

Cellular and Molecular Properties of Neurons

Inhibitory synaptic transmission is impaired in the Kölliker-Fuse of male, but not female, Rett syndrome mice

Jessica R. Whitaker-Fornek,^{1,2} Paul M. Jenkins,^{1,3} and Erica S. Levitt^{1,2,4}

¹Department of Pharmacology, University of Michigan Medical School, Ann Arbor, Michigan, United States; ²Department of Pharmacology and Therapeutics, University of Florida, Gainesville, Florida, United States; ³Department of Psychiatry, University of Michigan Medical School, Ann Arbor, Michigan, United States; and ⁴Department of Anesthesiology, University of Michigan Medical School, Ann Arbor, Michigan, United States

Abstract

Rett syndrome (RTT) is a severe neurodevelopmental disorder that mainly affects females due to silencing mutations in the X-linked *MECP2* gene. One of the most troubling symptoms of RTT is breathing irregularity, including apneas, breath-holds, and hyperventilation. Mice with silencing mutations in *Mecp2* exhibit breathing abnormalities similar to human patients and serve as useful models for studying mechanisms underlying breathing problems in RTT. Previous work implicated the pontine, respiratory-controlling Kölliker-Fuse (KF) in the breathing problems in RTT. The goal of this study was to test the hypothesis that inhibitory synaptic transmission is deficient in KF neurons from symptomatic male and female RTT mice. We performed whole cell voltage-clamp recordings from KF neurons in acute brain slices to examine spontaneous and electrically evoked inhibitory post-synaptic currents (IPSCs) in RTT mice and age- and sex-matched wild-type mice. The frequency of spontaneous IPSCs was reduced in KF neurons from male RTT mice but surprisingly not in female RTT mice. In addition, electrically evoked IPSCs were less reliable in KF neurons from male, but not female, RTT mice, which was positively correlated with paired-pulse facilitation, indicating decreased probability of release. KF neurons from male RTT mice were also more excitable and exhibited shorter-duration action potentials. Increased excitability of KF neurons from male mice was not explained by changes in axon initial segment length. These findings indicate impaired inhibitory neurotransmission and increased excitability of KF neurons in male but not female RTT mice and suggest that sex-dependent mechanisms contribute to breathing problems in RTT.

NEW & NOTEWORTHY Kölliker-Fuse (KF) neurons in acute brain slices from male Rett syndrome (RTT) mice receive reduced inhibitory synaptic inputs compared with wild-type littermates. In female RTT mice, inhibitory transmission was not different in KF neurons compared with controls. The results from this study show that sex-specific alterations in synaptic transmission occur in the KF of RTT mice.

electrophysiology; GABA; *Mecp2*; pons; respiration

INTRODUCTION

Rett syndrome (RTT) is a rare neurodevelopmental disorder that mainly affects girls and women (1). One of the most concerning symptoms of RTT is unpredictable, irregular breathing. Patients with RTT exhibit breath holding, hyperventilation, apnea, apneusis, and other breathing abnormalities (2, 3). Breathing problems disrupt daily activities such as eating and physical therapy sessions and sometimes lead to sudden death (4–7).

RTT is caused by silencing mutations in the X-linked gene *MECP2* that encodes methyl-CpG binding protein 2 (8). Like human patients with RTT, mice with loss-of-function mutations in the *Mecp2* gene exhibit breathing abnormalities (9, 10). Respiratory disturbances are very severe in male RTT mice that completely lack *Mecp2* protein (11, 12). Female RTT mice also have breathing problems that arise developmentally later compared with males, likely due to mosaic expression of functional *Mecp2* protein as a result of partial X inactivation (13–17). Male and female RTT mice are useful



models for uncovering dysfunction within the brainstem respiratory control network that underlies breathing irregularity in RTT.

Respiratory-controlling Kölliker-Fuse (KF) neurons have been implicated in the breathing irregularities shown in male (18) and female RTT mice (13, 19). KF neurons are located in the dorsolateral pons where they contribute to the control of breathing and upper airway patency (20–22). The KF supplies glutamatergic inputs to many downstream targets including respiratory rhythm and pattern-generating neurons in the medulla (23, 24). KF neuron activation enhances the postinspiratory phase of breathing resulting in a transient apnea (25–27). These apneas are similar to what is observed in RTT mice (13). In male RTT mice, inhibitory neurotransmission in other respiratory-related areas in the medulla is deficient (28, 29). Therefore, deficient inhibitory transmission onto KF neurons has been hypothesized to contribute to apneas in RTT mice (19).

Abdala et al. (19) investigated whether deficient inhibition in the KF contributed to increased postinspiratory activity and breathing irregularity in female RTT mice. Indeed, enhancing GABA levels in the KF by microinjection of a GABA reuptake inhibitor decreased apneas observed in recordings of respiratory motor output from female RTT mice (19). In addition, the number of GABAergic neurites is reduced in the KF of RTT mice (19). Together, these results suggest that respiratory-controlling KF neurons receive fewer inhibitory inputs in female RTT mice. Yet, Abdala and colleagues did not directly measure inhibitory synaptic transmission and excitability of neurons in the KF of RTT mice. Therefore, the goal of this research was to examine inhibitory synaptic transmission and action potential properties of neurons in the KF of symptomatic male and, importantly, female RTT mice. We used acute brain slice electrophysiology to test the hypothesis that inhibitory synaptic transmission is reduced in the KF of male and female RTT mice. We found that inhibitory neurotransmission was impaired in male, but surprisingly not female RTT mice. These results suggest that multiple synaptic mechanisms may be involved in a sex-specific manner in the breathing abnormalities observed in RTT.

METHODS

Animals

All experiments were approved by the University of Florida or the University of Michigan Institutional Animal Care and Use Committee (IACUC). All procedures using animals were in accordance with the National Institutes of Health Guide for the Care and Use of Laboratory Animals. Female heterozygous *Mecp2* knockout mutation mice, B6.129P2(C)-*Mecp2*^{tm1.1Bird} (Stock No. 003890, Jackson Labs, Bar Harbor, ME) were purchased from Jackson Labs and backcrossed with male wild-type C57Bl/6J mice for three generations to establish the colony, then maintained by crossing wild-type males from the colony. 4- to 6-wk-old *Mecp2*^{Bird/y} mice (male RTT mice) and 6- to 10-mo-old (average age = 227 ± 9 days) *Mecp2*^{Bird/+} mice (female RTT mice) were used for all experiments. Hindlimb clasping was observed in all RTT mice used for the experiments in this study.

Age and sex-matched wild-type littermates were used as controls.

Electrophysiology

Acute brain slices containing Kölliker-Fuse (KF) neurons were prepared as previously described (30). Briefly, mice were anesthetized with isoflurane just before decapitation and brain removal. To acquire KF-containing slices, the brain was blocked and mounted caudal end up in a vibratome chamber (Leica VT 1200S). Coronal slices (230 μm) were collected beginning at the caudal extent of the KF through the rostral extent of the KF. Brain slices were stored in warm (~32°C), oxygenated (95% O₂, 5% CO₂) artificial cerebrospinal fluid (aCSF) containing (in mM) 126 NaCl, 2.5 KCl, 1.2 MgCl₂, 2.6 CaCl₂, 1.2 NaH₂PO₄, 11 D-glucose, and 21.4 NaHCO₃. MK-801 (10 μM) was added to the cutting and slice storage solution to prevent excitotoxicity. Following at least 30 min of incubation, slices were placed into a recording chamber and perfused with warm (34°C) oxygenated aCSF with a flow rate of 1.5–3 mL/min.

Cells were visualized using an upright microscope (Nikon FN1) equipped with a custom-built IR-Dodt gradient contrast illumination and DAGE-MTI IR-2000 camera. KF neurons were located just ventral and lateral to the superior cerebellar peduncle.

Whole-cell voltage-clamp recordings were made from KF neurons using a Multiclamp 700B amplifier ($V_{\text{hold}} = -60$ mV). Glass recording pipettes (1.7–3 MΩ) were filled with high chloride internal solution containing (in mM): 115 KCl, 20 NaCl, 1.5 MgCl₂, 5 HEPES (K), 2 BAPTA, 1–2 Mg-ATP, 0.2 Na-GTP, adjusted to pH 7.35 and 275–285 mosM. The liquid junction potential (10 mV) was not corrected. Data were low-pass filtered at 10 kHz and collected at 20 kHz with pClamp 10.7 (Molecular Devices, Sunnyvale, CA), or collected at 400 Hz with PowerLab (LabChart version 5.4.2; AD Instruments, Colorado Springs, CO). Series resistance was monitored without compensation and remained <20 MΩ for inclusion. Current-clamp mode was used to record action potential firing following current injection (+200 pA, 500 ms step duration).

GABAergic and glycinergic inhibitory post-synaptic currents (IPSCs) were isolated using the glutamate receptor blockers DNQX (10 μM) in the perfusate and pre-treatment with MK-801 (10 μM) in the cutting solution. Electrically evoked IPSCs (eIPSCs) were elicited using a bipolar stimulating electrode placed in the KF. Stimulation trials consisted of 20 sweeps of paired electrical pulses (0.2-ms duration, 50-ms interpulse interval) that were delivered every 20 s. Stimulation intensity (10–50 μA) was adjusted to evoke a submaximal postsynaptic current. In a subset of experiments, the glycine receptor antagonist strychnine (1 μM) and the GABA_A receptor antagonist gabazine (1 μM) were applied to ensure all currents were blocked.

We did not differentiate spontaneous release from action-potential independent release. In a subset of experiments, we added TTX (1 μM) and found that this had no effect on IPSC frequency. The average frequency of glycinergic sIPSCs (4 ± 0.82 Hz, $n = 16$) was not different than glycinergic miniature-post-synaptic currents (5 ± 1.1 Hz, $n = 11$) (unpaired *t* test, $P = 0.3849$). The average frequency of GABAergic

sIPSCs (8 ± 1.1 Hz, $n = 18$) was not different than GABAergic miniature-post-synaptic currents (8 ± 2 Hz, $n = 10$) (unpaired t test, $P = 0.7755$). The majority of sIPSCs were likely action-potential independent.

Drugs

All blockers were reconstituted and stored according to manufacturer's instructions. (+)-MK-801 hydrogen maleate (Product No. M108), DNQX (Product No. D0540) and strychnine hydrochloride (Product No. S8753) were from Sigma-Aldrich. SR 95531 hydrobromide (Gabazine) was from Tocris Biosciences (Cat. No. 1262). Fresh solutions at the appropriate final concentrations were made fresh daily from concentrated stock solutions.

Immunohistochemistry

Mice were deeply anesthetized with isoflurane and transcardially perfused with ice-cold phosphate-buffered saline (PBS) followed by 10% formalin. Brains were removed and placed in 10% formalin for 24 h before immersion in 20% sucrose overnight and 30% sucrose for ~ 6 h. Cryoprotected brains were frozen in optimal cutting temperature (OCT) compound (Fisher Tissue Plus) on dry ice and stored at -80°C . Coronal brain slices (40- μm thick) containing the KF were cut using a Leica cryostat and stored as free-floating sections in PBS at 4°C . Brain slices were permeabilized using PBS containing 0.3% Triton-X-100 (PBS-T) and blocked for 1 h with a buffer solution containing (3% normal goat serum and 2% bovine serum albumen) and incubated overnight at 4°C with primary antibody rabbit anti-ankyrin G (laboratory-generated, 1:1,000) (31) diluted with blocking buffer. Brain slices were rinsed with PBS-T and incubated with secondary antibody goat anti-rabbit Alexa Fluor 647 (Invitrogen, AE32733, 1:500) diluted with a blocking buffer for 1.5 h at room temperature. Finally, slices were rinsed with PBS-T and mounted on slides with Fluoromount G with DAPI mounting media (Invitrogen). Brain slices containing KF neurons were imaged using a Zeiss LSM 880 confocal microscope equipped with Airyscan processing. Immunostaining experiments were performed in parallel on brain slices from six, 6-wk-old male mice ($n = 3$ RTT, $n = 3$ WT littermates). The KF area from WT and RTT mouse brains ($n = 6$ mice; 3 images per mouse) were immunostained and imaged in parallel with a 63X NA1.4 Oil/DIC Plan-Apochromat objective and 633 nm lasers. Images were pseudocolored white. As a control, a subset of brain slices were incubated only with a secondary antibody to validate the specificity of the primary antibody.

Axon Initial Segment Quantification

Z stacks (20 μm , 10 slices) were collapsed to create maximum intensity z projections in Fiji (32). The segmented line measure tool was used to acquire a fluorescence profile along the length of the axon initial segment (AIS). The start and end of the AIS were defined as 15% of the maximum fluorescence value. AIS length was measured as the distance between the start and end of the AIS. Normalized (i.e., background subtracted) mean fluorescence intensity for the total ankyrin-G signal was calculated in Fiji for each maximum intensity z projection taken of the KF area ($n =$

8 images from 3 RTT mice, $n = 9$ images from 3 wild-type littermates).

Data Analysis

Spontaneous IPSCs were detected and analyzed for 5-min epochs during baseline and following drug exposure (Clampfit 11.1, Molecular Devices). For electrically-evoked IPSCs, the average amplitude and decay tau of the first eIPSC of the pair were calculated from the averaged waveform for 20 sweeps. Paired-pulse ratio was determined by dividing the average amplitude of the second eIPSC by the average amplitude of the first eIPSC (P2/P1). The failure rate for the first eIPSC of the pair (i.e., the percentage of stimulations that failed to evoke a postsynaptic current) was calculated by dividing the number of failed stimulations by the total number of stimuli (20) and multiplying by 100. The average action potential firing frequency was calculated using the action potential search mode in Clampfit. The average action potential waveform per neuron was used to calculate action potential half-width (duration at 50% of peak), rise time (75 to 15% of peak), decay time (10% to 90% of peak), after-hyperpolarization (difference from baseline) and overshoot.

All statistical analyses were performed using GraphPad Prism (version 9). All error bars represent SE unless otherwise stated. Replicates are individual neurons. One to two neurons were recorded per animal. Data were tested for normality with D'Agostino–Pearson tests. Comparisons between the two groups were made using unpaired t test for normally distributed data or Mann–Whitney U test for non-normally distributed data.

RESULTS

To examine inhibitory synaptic transmission in the respiratory-controlling KF area of symptomatic male and female RTT mice, we made whole cell voltage-clamp recordings from KF neurons contained in acute brain slices from male hemizygous *Mecp2*^{Bird/y} mice (male RTT mice), female heterozygous *Mecp2*^{Bird/+} mice (female RTT mice) and their age- and sex-matched wild-type littermates. Male hemizygous *Mecp2*^{Bird/y} mice (male RTT mice) are null for *Mecp2* function, given *Mecp2* is X-linked. Males exhibit severe respiratory and motor deficits by 4 wk of age, with a lifespan of 50–60 days (10). Therefore, 4- to 6-wk-old male mice were used for all experiments. Female, heterozygous *Mecp2*^{Bird/+} mice (female RTT mice) display respiratory problems at 6 mo of age or older (15). Therefore, 6- to 10-mo-old adult female mice (average age = 227 ± 9 days) were used for experiments.

Spontaneous Inhibitory Postsynaptic Currents Are Less Frequent in KF Neurons from Male RTT Mice

We measured spontaneous inhibitory postsynaptic currents (sIPSCs) from KF neurons in brain slices from male RTT mice and age-matched wild-type littermate controls (Fig. 1A). The frequency of sIPSCs was significantly reduced in male RTT mice compared with wild-type mice (Fig. 1B; $P = 0.0012$, unpaired t test). However, the amplitude of sIPSCs was not different for KF neurons from male RTT mice compared with wild-type littermates (Fig. 1C; $P = 0.1151$, unpaired t test). Differences in the decay kinetics of sIPSCs often indicate differences in receptor subunit composition

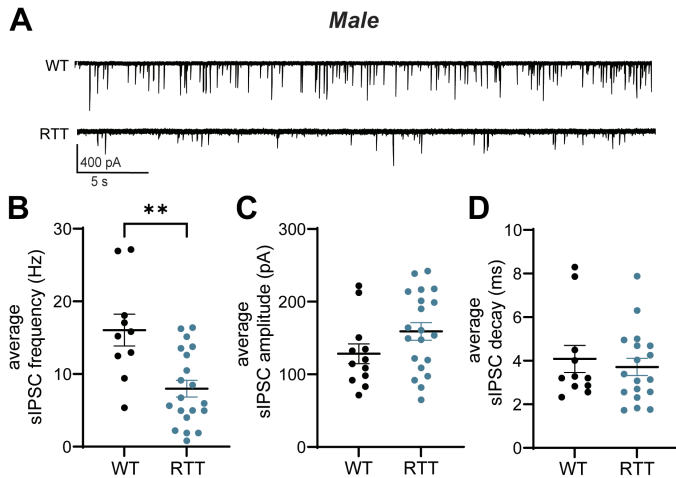


Figure 1. Spontaneous inhibitory synaptic transmission in Kölliker-Fuse (KF) neurons from male Rett syndrome (RTT) mice. **A:** representative traces of spontaneous inhibitory postsynaptic currents (sIPSCs) recorded from KF neurons contained in brain slices from male RTT mice and age-matched wild-type (WT) littermates. **B:** the frequency of sIPSCs was reduced in KF neurons from RTT mice compared with controls (** $P = 0.0012$, unpaired t test). **C:** there was no difference in the amplitude of sIPSCs ($P = 0.1151$, unpaired t test). **D:** the average decay tau of sIPSCs was not different for KF neurons from male RTT mice compared with controls ($P = 0.8631$, Mann–Whitney test). Line and error bars indicate means \pm SE. Individual data points are from individual neurons, 1–2 neurons per mouse.

(33). There was no difference in the decay tau for sIPSCs from KF neurons from male RTT mice compared with WT controls (Fig. 1D; $P = 0.8631$, Mann–Whitney test). In a subset of experiments, co-application of gabazine (1 μ M) and strychnine (1 μ M) eliminated all sIPSCs (average frequency = 0 Hz, $n = 4$ cells from 3 animals), confirming IPSCs were due to GABA_A and glycine receptor activation, respectively.

Spontaneous Inhibitory Postsynaptic Currents Are Not Different in KF Neurons from Female RTT Mice

To examine inhibitory synaptic transmission in the KF of female RTT mice, we performed whole cell voltage clamp recordings from KF neurons contained in brain slices from female RTT mice and age-matched wild-type littermate controls (Fig. 2A). In KF neurons from WT female mice, the average frequency of sIPSCs was lower compared with WT males ($P = 0.0023$, unpaired t test). In contrast to male RTT mice, the frequency of sIPSCs was not different for RTT females compared with wild-type littermates (Fig. 2B; $P = 0.4668$, Mann–Whitney test). The amplitude of sIPSCs was also not different for KF neurons from female RTT mice compared with wild-type controls (Fig. 2C; $P = 0.4018$, unpaired t test). The decay tau was also not different for sIPSCs female RTT mice compared with wild-type littermates (Fig. 2D; $P = 0.2918$, Mann–Whitney test). These results suggest that spontaneous inhibitory transmission is not impaired in KF neurons from female RTT mice.

Since we used a wide age range of female mice (6–10 mo), we also wanted to determine if there was an association between age and sIPSC frequency. There was no correlation between age and sIPSC frequency in female RTT mice or female WT mice ($P = 0.7621$ for RTT mice; $P = 0.3267$ for WT mice; linear regression).

Evoked Inhibitory Synaptic Currents in KF Neurons from Male Mice

To investigate responses to stimulated GABA and glycine release in the KF, we delivered paired electrical stimuli to the KF to evoke inhibitory postsynaptic currents (eIPSCs) in KF neurons from male RTT mice and wild-type littermates (Fig. 3A). We measured the amplitude and kinetics of the eIPSC evoked by the first stimulus pulse. There was no difference in eIPSC amplitude for KF neurons from male RTT mice compared with wild-type controls (Fig. 3B; $P = 0.1453$, unpaired t test). There was also no difference in the decay tau of eIPSCs for KF neurons from male mice (Fig. 3C; $P = 0.8902$, unpaired t test). In a subset of experiments, we confirmed that co-application of strychnine (1 μ M) and gabazine (1 μ M) blocked electrically evoked currents (average peak amplitude: 10.8 ± 2.9 pA, $n = 4$ cells from 3 animals).

Electrical stimulation did not always evoke an IPSC on every sweep. For the first pulse, we determined the percentage of stimulations that failed to evoke an IPSC by dividing the number of failed stimulations by the total number of stimulation trials [(number of failed stimulations/total number of stimulation trials) \times 100] (Fig. 3D). In wild-type mice, eIPSCs were elicited by the first stimulation pulse in all KF neurons with a low failure rate of 19% (Fig. 3D). There were significantly more failures to evoke an IPSC on the first pulse for KF neurons from male RTT mice compared with controls ($P = 0.0219$, unpaired t test), despite the fact that stimulation intensity did not differ between genotypes ($P = 0.3702$, Mann–Whitney test). In RTT mice, there was a large range of failure rates including three neurons from three different mice where the first stimulation pulse completely failed to

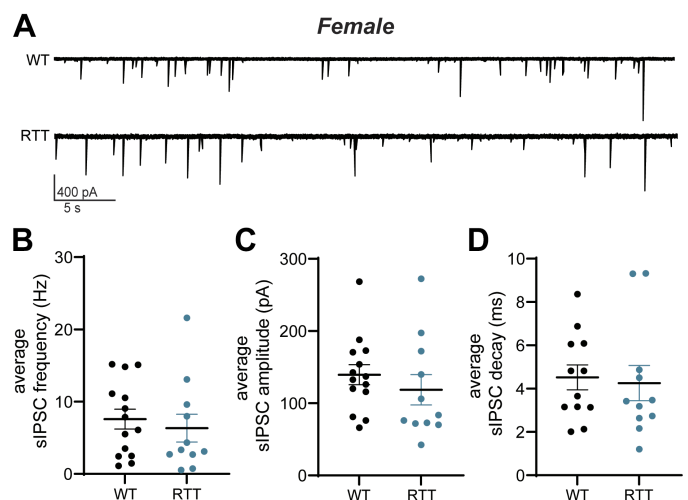


Figure 2. Spontaneous inhibitory synaptic transmission in Kölliker-Fuse (KF) neurons from female Rett syndrome (RTT) mice. **A:** representative traces of spontaneous inhibitory postsynaptic currents (sIPSCs) recorded from KF neurons contained in brain slices from female RTT mice and age-matched wild-type (WT) littermates. **B:** in contrast to males, sIPSC frequency was not different in female RTT mice compared with controls ($P = 0.4668$, Mann–Whitney test). **C:** the average sIPSC amplitude was not different in female RTT mice compared with controls ($P = 0.4018$, unpaired t test). **D:** the average sIPSC decay tau was not different for female RTT mice compared with controls ($P = 0.2918$, unpaired t test). Line and error bars indicate means \pm SE. Individual data points are from individual neurons, 1–2 neurons per mouse.

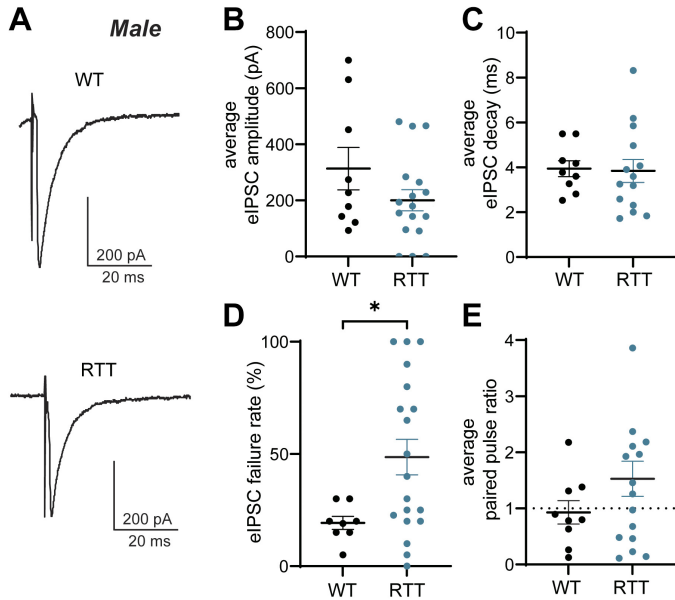


Figure 3. Evoked inhibitory synaptic transmission in Kölliker-Fuse (KF) neurons from male Rett syndrome (RTT) mice. **A:** representative traces of electrically evoked inhibitory postsynaptic currents (eIPSCs) recorded from KF neurons from male RTT mice and wild-type (WT) controls. The average eIPSC amplitude (**B**) and decay tau (**C**) for male RTT mice were not different from controls (amplitude: $P = 0.1453$; decay tau: $P = 0.8902$, unpaired t tests). **D:** the percentage of stimulations that failed to evoke an IPSC was higher in male RTT mice compared with controls ($*P = 0.0219$, unpaired t test). **E:** the paired-pulse ratio for male RTT mice was not different from WT controls ($P = 0.1957$). Line and error bars indicate means \pm SE. Individual data points are from individual neurons, 1–2 neurons per mouse.

elicit IPSCs. In all three of those instances, the second stimulation elicited an IPSC. Therefore, we examined the paired pulse ratio (PPR) for KF neurons from wild-type and RTT mice (average amplitude of the eIPSC for pulse 2/average amplitude of the eIPSC for pulse 1) (Fig. 3E).

Both paired-pulse facilitation and paired-pulse depression were observed for eIPSCs from KF neurons from wild-type male mice. A greater range of PPR values was observed for eIPSCs for KF neurons from male RTT mice, and there was a greater proportion of neurons with paired-pulse facilitation in RTT male mice (8 out of 15) versus WT male mice (3 out of 9). However, there was no significant difference in the average PPR for eIPSCs from RTT versus WT mice ($P = 0.196$, unpaired t test). Since paired-pulse facilitation indicates a lower probability of release on the first pulse, we examined the relationship between PPR and failure rate. In RTT mice, the increased failure rate was significantly correlated with increased PPR ($P = 0.0011$, linear regression). Together, these data suggest that the probability of release is reduced in neurons from male RTT mice since failure rate and paired-pulse facilitation both indicate decreased probability of release.

Evoked Inhibitory Synaptic Currents in KF Neurons from Female Mice

Electrically evoked IPSCs (eIPSCs) were recorded from KF neurons in brain slices from female RTT mice and age-matched wild-type littermates (Fig. 4A). There was no difference in the amplitude of eIPSCs in KF neurons from female

RTT mice compared with wild-type controls (Fig. 4B; $P = 0.7939$, unpaired t test). The decay tau of eIPSCs was also not different for female RTT mice compared with wild-type controls (Fig. 4C; $P = 0.1061$, unpaired t test). Similar to males, there was no difference in stimulus intensity used to evoke IPSCs in KF neurons from female RTT mice compared with controls ($P = 0.4105$, Mann-Whitney test).

Paired-pulse ratio and the percentage of failures were examined as an indicator of GABA and glycine release properties. Similar to males, eIPSCs showed both paired-pulse facilitation and depression (Fig. 4E) and there was no difference in the paired-pulse ratio ($P = 0.8562$, Mann-Whitney test). Failures to evoke IPSCs were also observed in KF neuron recordings from female RTT and wild-type mice (Fig. 4D). However, there was no difference in the percentage of failures for eIPSCs in KF neurons from female mice ($P = 0.8966$, unpaired t test). Thus, unlike males, there were no differences observed in electrically evoked release properties of inhibitory neurotransmitters in the KF of female RTT mice compared with wild-type controls.

Action Potential Properties of KF Neurons from Male Mice

The excitability of KF neurons in response to depolarizing current injections was examined at the beginning of all experiments. No KF neurons from either genotype showed spontaneous action potential firing at baseline, consistent

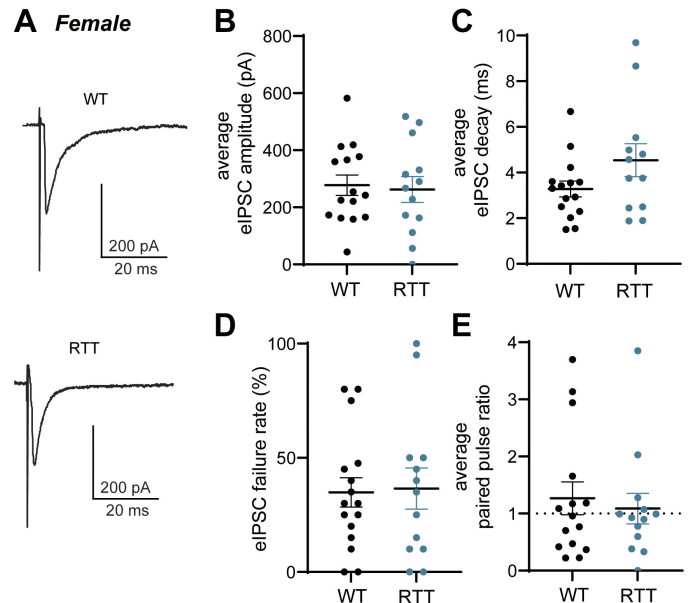


Figure 4. Evoked inhibitory synaptic transmission in Kölliker-Fuse (KF) neurons from female Rett syndrome (RTT) mice. **A:** representative traces of electrically evoked inhibitory postsynaptic currents (eIPSCs) recorded from KF neurons from female RTT mice and wild-type (WT) controls. Summarized data for the average eIPSC amplitude (**B**), decay tau (**C**) for female RTT mice were not different from controls (amplitude: $P = 0.7939$; decay tau: $P = 0.1061$; unpaired t tests). **D:** in contrast to males, no significant differences were observed for the percentage of failed eIPSCs in female RTT mice compared with WT controls ($P = 0.8966$, unpaired t test). **E:** the average paired-pulse ratio was not different for female RTT mice compared with controls ($P = 0.8562$, Mann-Whitney test). Line and error bars indicate means \pm SE. Individual data points are from individual neurons, 1–2 neurons per mouse.

with previous studies (30). KF neurons from both male RTT mice and wild-type littermates fired action potentials as a result of depolarizing current injections (200 pA, 500 ms) (Fig. 5A). KF neurons from male RTT mice fired action potentials at a higher average frequency compared to WT littermates (Fig. 5B, $P = 0.0413$, Mann-Whitney test). Consistent with higher frequency firing, the action potential half-width was shorter for KF neurons from male RTT mice compared with controls (Fig. 5C, $P = 0.0087$, Mann-Whitney test). Although the rise time for action potentials was not different (Fig. 5D, $P = 0.0726$, Mann-Whitney test), the difference in duration was due to faster decay times in KF neurons from male RTT mice (Fig. 5E, $P = 0.0039$, Mann-Whitney test). There was also no difference in the action potential overshoot for male RTT mice compared with wild-type male mice (WT: 50 ± 4 mV, $n = 8$; RTT: 47 ± 2 mV, $n = 23$; unpaired t test, $P = 0.5365$). The after-hyperpolarization was also not different for action potentials fired by KF neurons from male RTT mice compared with controls (WT: 20 ± 3 mV, $n = 8$; RTT: 23 ± 1 mV, $n = 23$; Mann-Whitney test, $P = 0.1102$).

Importantly, there was no difference in the resting membrane potential of KF neurons from male RTT mice compared to WT mice (WT: -56 ± 3 mV, $n = 7$; RTT: -57 ± 2 mV, $n = 23$; Mann-Whitney test, $P = 0.6402$). There was no difference in input resistance for KF neurons from male RTT mice compared with male WT mice (WT: 661 ± 90 M Ω ; RTT: 561 ± 38 M Ω ; unpaired t test, $P = 0.2409$). Therefore, the increased firing rate in response to depolarization cannot be

explained by differences in input resistance or resting membrane potential, and likely reflect intrinsic properties of the neuron.

Axon Initial Segment Length in KF Area from Male Mice

Neuronal excitability and firing properties are influenced by the structural properties of the axon initial segment (AIS) (34). Therefore, we immunofluorescently labeled ankyrin-G, the scaffolding protein responsible for the organization of the ion channels necessary for action potential initiation at the AIS (35), to examine the AIS length in KF neurons from male RTT mice and wild-type littermates (Fig. 6A). We found there was no difference in average AIS length for KF neurons from male RTT mice compared with controls (Fig. 6B, $P = 0.2398$, Mann-Whitney test). There was also no effect of genotype on the mean fluorescence intensity of ankyrin-G immunostaining in the KF area [$P = 0.5159$, unpaired t test, $n = 6$ mice (3 WT, 3 RTT), 2 or 3 images per mouse].

Action Potential Properties of KF Neurons from Female Mice

Similar to males, action potentials were elicited in KF neurons from female RTT mice and wild-type littermates in response to depolarizing current (500-ms duration, 200 pA) (Fig. 7A). In contrast to males, there were no differences in action potential firing frequency for KF neurons from female RTT mice compared with wild-type littermates (Fig. 7B, $P = 0.7373$, unpaired t test). There were also no differences in action potential half-width (Fig. 7C, $P = 0.7433$, Mann-Whitney test), average rise time (Fig. 7D, $p = 0.3929$, Mann-Whitney test), or average decay time (Fig. 7E, $P = 0.9680$, Mann-Whitney test) for KF neurons from female RTT mice compared with controls. There was also no difference in action potential overshoot for female RTT mice compared with wild-type female mice (WT: 46 ± 2 mV, $n = 15$; RTT: 45 ± 3 mV, $n = 7$; Mann-Whitney test, $P = 0.8557$). The after-hyperpolarization was also not different for action potentials fired by KF neurons from female RTT mice compared with controls (WT: 25 ± 2 mV, $n = 15$; RTT: 25 ± 6 mV, $n = 7$; Mann-Whitney test, $P = 0.99$).

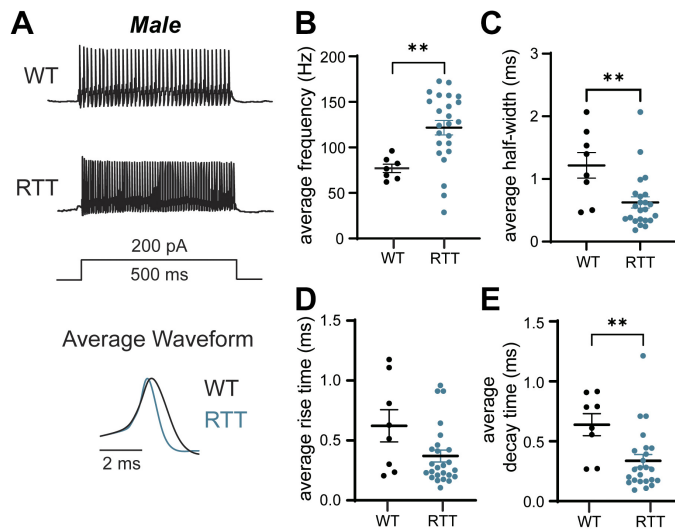


Figure 5. Firing properties of Kölliker-Fuse (KF) neurons from male Rett syndrome (RTT) mice. **A:** representative whole cell current clamp recordings from KF neurons from a wild-type (WT) male mouse (top trace) and a RTT male mouse (bottom trace). Average action potential waveforms are overlaid below. Summary of average action potential firing frequency (**B**), action potential half-width (**C**), average rise time (**D**), and average decay time (**E**). KF neurons from male RTT mice fired higher-frequency action potentials compared to wild-type controls (**B**) (** $P = 0.0038$, Mann-Whitney test). The average action potential half-width was shorter for KF neurons from RTT mice (**C**) (** $P = 0.0087$, Mann-Whitney test). Action potentials fired by KF neurons from RTT mice did not have significantly faster rise times (**D**) (** $P = 0.0726$, Mann-Whitney test) but decay times were significantly faster compared with controls (**E**) (** $P = 0.0039$, Mann-Whitney test). Line and error bars indicate means \pm SE. Individual data points are from individual neurons, 1–2 neurons per mouse.

DISCUSSION

This study examined spontaneous and evoked inhibitory synaptic transmission in KF neurons from symptomatic male and female RTT mice in comparison with their wild-type, age-, and sex-matched littermates. In male RTT mice, we show that KF neurons exhibit deficient inhibitory synaptic transmission and increased excitability. Deficient inhibitory synaptic transmission appears to be due to deficits in neurotransmitter release, since the frequency, but not amplitude, of spontaneous IPSCs was reduced and stimulation-evoked IPSCs were less reliably elicited, which was associated with paired-pulse facilitation. However, in female RTT mice, we show there are no differences in the synaptic inhibitory transmission onto KF neurons or action potential firing properties of KF neurons compared with control age- and sex-matched wild-type littermates. This is an important sex difference since RTT primarily affects females, but much of the work on synaptic transmission in RTT mouse models has used male mice (28, 29, 36).

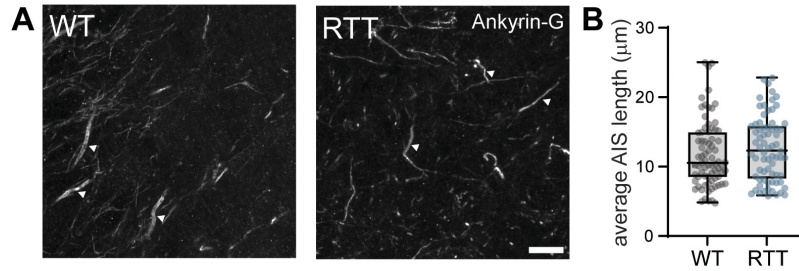


Figure 6. Axon initial segments in the Kölliker-Fuse (KF) area from male Rett syndrome (RTT) mice. *A*: representative maximum intensity z projection images ($\times 60$ magnification) showing ankyrin-G immunostaining in the KF area from a male wild-type (WT) and male RTT mouse. Ankyrin-G staining was used to visualize axon initial segments (AIS; white arrows denote three examples per image). Scale bar = 10 μm . *B*: average length of the AIS was not different for male RTT mice compared with WT controls ($P = 0.2398$, Mann–Whitney test, $n = 6$ mice (3 WT, 3 RTT), 2–3 images per mouse). Box and whisker plots indicate median and quartile ranges including the minimum and maximum values for individual segments (individual data points).

Our findings for KF neurons from male RTT mice add to growing evidence in support of impaired inhibitory synaptic transmission within the brainstem breathing control network of male RTT mice (36). GABAergic/glycinergic sIPSC frequency is also decreased in rostroventrolateral medullary neurons and the nucleus of the solitary tract neurons from male RTT mice (28, 29). The source of the impaired inhibitory input is yet to be identified. The KF receives inhibitory inputs from brainstem regions such as the nucleus of the solitary tract (37, 38), the Bötzinger complex (39) and the preBötzinger complex (40). In addition, inhibitory inputs onto lateral parabrachial neurons, also part of the pontine respiratory group, also come from forebrain regions, such as

the central nucleus of the amygdala (41). Which, if any, of these regions account for the reduction in inhibitory transmission we observed in KF neurons from male RTT mice remains to be determined. Given the widespread impairment of inhibitory neurotransmission in the brainstem, it is likely that multiple regions contribute. The variability of evoked IPSC failure rate and paired-pulse ratio we observed in male RTT mice suggests that impairments onto KF neurons could be input and/or neuron specific.

We also show that KF neurons from male RTT mice fire higher frequency action potentials which is similar to the hyperexcitability present in medullary respiratory neurons (42) and mesencephalic trigeminal neurons (43) from male RTT rodent models. Hyperexcitability can occur due to the structural plasticity of the axon initial segment where action potentials are initiated (34). Increased length of axon initial segments is found in hippocampal neurons in a mouse model of Angelman Syndrome (35, 44). However, differences in axon initial segment length did not explain the hyperexcitability of KF neurons from male RTT mice in our study. Other properties of the AIS, such as increased voltage-gated potassium channel expression (45), may contribute to the shorter duration of action potentials we observed in KF neurons from male RTT mice.

Our results from female mice are unexpected given previously published data from Abdala et al., who showed that the number of GABAergic neurites is reduced in the KF area of female RTT mice compared with wild-type littermates (19). In addition, blocking GABA reuptake locally within the KF decreases apneas in the in situ working heart brainstem preparation of female RTT mice (19). Yet, we found no physiological evidence in support of deficient GABAergic synaptic transmission in the KF of female RTT mice. The different findings can be explained by the approaches we used to study inhibitory synaptic transmission onto KF neurons. First, we directly measured inhibitory synaptic transmission onto KF neurons using ex vivo electrophysiology, rather than indirectly by visualizing GABAergic projections using green fluorescent protein expression driven by the Gad67 promoter which is an anatomical proxy for GABA-producing neurons. Second, an alternate explanation for the positive effects of the GABA reuptake inhibitor (19) could be the restoration of excitatory/inhibitory balance that was disrupted due to excessive excitatory transmission, rather than deficient inhibitory transmission, in the KF of RTT mice. To test

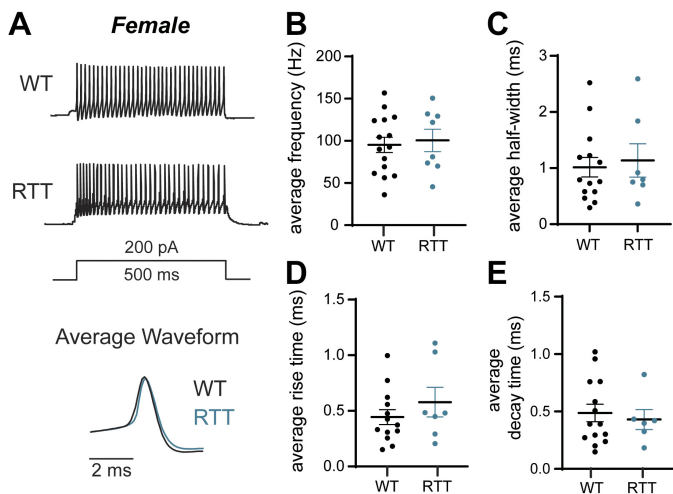


Figure 7. Firing properties of Kölliker-Fuse (KF) neurons from female Rett syndrome (RTT) mice. *A*: representative whole cell current clamp recordings from KF neurons from a wild-type (WT) female mouse (top trace) and an RTT female mouse (bottom trace). The average action potential waveforms are overlaid below. Summary of average action potential firing frequency (*B*), action potential half-width (*C*), average rise time (*D*), and average decay time (*E*). Action potentials fired by KF neurons from female RTT mice were no different than wild-type controls. There was no difference in the frequency of action potentials compared to wild-type controls (*B*) ($P = 0.7373$, unpaired t test). The average action potential half-width was not different for KF neurons from RTT mice (*C*) ($P = 0.7433$, Mann–Whitney test). Also, there were no differences in the rise time ($P = 0.3929$, Mann–Whitney test) or decay time ($P = 0.9680$, Mann–Whitney test) for action potentials fired by KF neurons from RTT mice. Line and error bars indicate means \pm SE. Individual data points are from individual neurons, 1–2 neurons per mouse.

this hypothesis, future experiments could measure spontaneous excitatory post-synaptic currents in KF neurons from female RTT mice. Finally, we used younger mice [6–10 mo vs. 14 ± 1 mo in Abdala et al. (19)], which was our feasibility limit for electrophysiology experiments. Although they were younger, the RTT mice we used were symptomatic and we did not observe age-related changes in inhibitory neurotransmission within this 6–10 mo range. We also have not observed any association between age and apnea incidence or breathing irregularity in 5- to 10-mo-old female *Mecp2*^{Bird/+} RTT mice (46). Regardless, we cannot rule out the possibility that at older ages (>10 mo) a difference in inhibitory neurotransmission would emerge. Interestingly, patients with RTT and RTT mouse models have age-related improvements in breathing (47–49), which does not support a later age-related decline in inhibitory neurotransmission in the KF underlying respiratory disturbances in RTT.

Limitations

The goal of the present study was to examine inhibitory synaptic currents in symptomatic male and, importantly, female RTT mice. Male RTT mice show breathing problems as early as 4–6 wk old, whereas female RTT mice show breathing irregularities once they reach 6 mo of age (15). The substantial age difference between male and female symptomatic mice complicates direct comparisons between the sexes in the present work. For example, we cannot rule out age as a contributing factor to lower sIPSC frequency in KF neurons from WT female mice compared with WT males (50). Future work examining synaptic transmission in female mice at presymptomatic ages could be informative to determine whether deficits are present earlier in development.

Second, we did not identify whether KF neurons from female RTT mice contained functional *Mecp2* protein. Due to partial X-inactivation, approximately half of KF neurons in female RTT mice are *Mecp2*-negative and half are *Mecp2*-positive (19). Both *Mecp2*-positive and *Mecp2*-negative KF neurons from female RTT mice were surrounded by significantly fewer GABAergic perisomatic bouton-like puncta compared with wild-type littermates (19). Therefore, although cell-autonomous effects are a possibility for some postsynaptic responses in RTT mice (51), we do not think that cell-autonomous effects of *Mecp2* expression in the postsynaptic neuron influenced inhibitory synaptic transmission onto KF neurons from female RTT mice in our study.

Conclusions

Breathing problems can be life-threatening for girls and women diagnosed with RTT. Uncovering the neural dysfunction in the brainstem respiratory control network of RTT mice is a critical first step toward learning how to correct breathing problems in patients with RTT. Using acute brain slice electrophysiology, we found that inhibitory synaptic transmission was impaired in the KF area of male RTT mice. Meanwhile, female RTT mice did not have decreased inhibitory transmission upon their KF neurons. The widespread imbalance of excitatory and inhibitory signaling in the brains of RTT mice poses a daunting challenge for restoring normal brain function and correcting the devastating neurological issues in human patients with RTT. Targeted

approaches are needed to restore excitation/inhibition balance across the breathing control network with the hope of improving the breathing abnormalities in RTT.

DATA AVAILABILITY

Data will be made available upon reasonable request.

ACKNOWLEDGMENTS

Thank you to Nicole Filipelli for technical assistance.

GRANTS

This work was funded by the International Rett Syndrome Foundation Basic Research Grant No. 3608 (to E.S.L.). The work was also supported by National Institute of Mental Health Grant R01MH126960 (to P.M.J.) and by National Institute on Drug Abuse Grant R01DA047978 (to E.S.L.).

DISCLOSURES

No conflicts of interest, financial or otherwise, are declared by the authors.

AUTHOR CONTRIBUTIONS

E.S.L. conceived and designed research; J.R.W.-F. performed experiments; J.R.W.-F. analyzed data; J.R.W.-F., P.M.J., and E.S.L. interpreted results of experiments; J.R.W.-F. prepared figures; J.R.W. drafted manuscript; P.M.J. and E.S.L. edited and revised manuscript; P.M.J. and E.S.L. approved final version of manuscript.

REFERENCES

- Ivy AS, Standridge SM. Rett syndrome: a timely review from recognition to current clinical approaches and clinical study updates. *Semin Pediatr Neurol* 37: 100881, 2021. doi:10.1016/j.spn.2021.100881.
- Ramirez JM, Karlen-Amarante M, Wang JJ, Huff A, Burgraff N. Breathing disturbances in Rett syndrome. *Handb Clin Neurol* 189: 139–151, 2022. doi:10.1016/B978-0-323-91532-8.00018-5.
- Ramirez JM, Karlen-Amarante M, Wang JJ, Bush NE, Carroll MS, Weese-Mayer DE, Huff A. The pathophysiology of rett syndrome with a focus on breathing dysfunctions. *Physiology (Bethesda)* 35: 375–390, 2020. doi:10.1152/physiol.00008.2020.
- Kerr AM, Armstrong DD, Prescott RJ, Doyle D, Kearney DL. Rett syndrome: analysis of deaths in the British survey. *Eur Child Adolesc Psychiatry* 6, Suppl 1: 71–74, 1997.
- Singh J, Lanzarini E, Santosh P. Autonomic dysfunction and sudden death in patients with Rett syndrome: a systematic review. *J Psychiatry Neurosci* 45: 150–181, 2020. doi:10.1503/jpn.190033.
- Tarquino DC, Hou W, Neul JL, Berkmen GK, Drummond J, Aronoff E, Harris J, Lane JB, Kaufmann WE, Motil KJ, Glaze DG, Skinner SA, Percy AK. The course of awake breathing disturbances across the lifespan in Rett syndrome. *Brain Dev* 40: 515–529, 2018. doi:10.1016/j.braindev.2018.03.010.
- Weese-Mayer DE, Lieske SP, Boothby CM, Kenny AS, Bennett HL, Silvestri JM, Ramirez JM. Autonomic nervous system dysregulation: breathing and heart rate perturbation during wakefulness in young girls with Rett syndrome. *Pediatr Res* 60: 443–449, 2006. doi:10.1203/01.pdr.0000238302.84552.d0.
- Amir RE, Van den Veyver IB, Wan M, Tran CQ, Francke U, Zoghbi HY. Rett syndrome is caused by mutations in X-linked MECP2, encoding methyl-CpG-binding protein 2. *Nat Genet* 23: 185–188, 1999. doi:10.1038/13810.
- Guy J, Hendrich B, Holmes M, Martin JE, Bird A. A mouse *Mecp2*-null mutation causes neurological symptoms that mimic Rett syndrome. *Nat Genet* 27: 322–326, 2001. doi:10.1038/85899.

10. **Viemari JC, Roux JC, Tryba AK, Saywell V, Burnet H, Peña F, Zanella S, Bévangut M, Barthelemy-Requin M, Herzing LB, Moncla A, Mancini J, Ramirez JM, Villard L, Hilaire G.** Mecp2 deficiency disrupts norepinephrine and respiratory systems in mice. *J Neurosci* 25: 11521–11530, 2005. doi:10.1523/JNEUROSCI.4373-05.2005.
11. **Katz DM, Dutschmann M, Ramirez JM, Hilaire G.** Breathing disorders in Rett syndrome: progressive neurochemical dysfunction in the respiratory network after birth. *Respir Physiol Neurobiol* 168: 101–108, 2009. doi:10.1016/j.resp.2009.04.017.
12. **Voituron N, Zanella S, Menuet C, Dutschmann M, Hilaire G.** Early breathing defects after moderate hypoxia or hypercapnia in a mouse model of Rett syndrome. *Respir Physiol Neurobiol* 168: 109–118, 2009. doi:10.1016/j.resp.2009.05.013.
13. **Abdala AP, Dutschmann M, Bissonnette JM, Paton JF.** Correction of respiratory disorders in a mouse model of Rett syndrome. *Proc Natl Acad Sci USA* 107: 18208–18213, 2010. doi:10.1073/pnas.1012104107.
14. **Bissonnette JM, Knopp SJ.** Effect of inspired oxygen on periodic breathing in methy-CpG-binding protein 2 (Mecp2) deficient mice. *J Appl Physiol* (1985) 104: 198–204, 2008. doi:10.1152/jappphysiol.00843.2007.
15. **Jiang C, Cui N, Zhong W, Johnson CM, Wu Y.** Breathing abnormalities in animal models of Rett syndrome a female neurogenetic disorder. *Respir Physiol Neurobiol* 245: 45–52, 2017. doi:10.1016/j.resp.2016.11.011.
16. **Levitt ES, Hunnicutt BJ, Knopp SJ, Williams JT, Bissonnette JM.** A selective 5-HT1a receptor agonist improves respiration in a mouse model of Rett syndrome. *J Appl Physiol* (1985) 115: 1626–1633, 2013. doi:10.1152/jappphysiol.00889.2013.
17. **Samaco RC, McGraw CM, Ward CS, Sun Y, Neul JL, Zoghbi HY.** Female Mecp2(+/-) mice display robust behavioral deficits on two different genetic backgrounds providing a framework for pre-clinical studies. *Hum Mol Genet* 22: 96–109, 2013. doi:10.1093/hmg/dd5406.
18. **Stettner GM, Huppke P, Brendel C, Richter DW, Gärtner J, Dutschmann M.** Breathing dysfunctions associated with impaired control of postinspiratory activity in Mecp2-ly knockout mice. *J Physiol* 579: 863–876, 2007. doi:10.1113/jphysiol.2006.119966.
19. **Abdala AP, Toward MA, Dutschmann M, Bissonnette JM, Paton JF.** Deficiency of GABAergic synaptic inhibition in the Kölliker-Fuse area underlies respiratory dysrhythmia in a mouse model of Rett syndrome. *J Physiol* 594: 223–237, 2016. doi:10.1113/JP270966.
20. **Dutschmann M, Herbert H.** The Kölliker-Fuse nucleus gates the postinspiratory phase of the respiratory cycle to control inspiratory off-switch and upper airway resistance in rat. *Eur J Neurosci* 24: 1071–1084, 2006. doi:10.1111/j.1460-9568.2006.04981.x.
21. **Dutschmann M, Dick TE.** Pontine mechanisms of respiratory control. *Compr Physiol* 2: 2443–2469, 2012. doi:10.1002/cphy.c100015.
22. **Varga AG, Maletz SN, Bateman JT, Reid BT, Levitt ES.** Neurochemistry of the Kölliker-Fuse nucleus from a respiratory perspective. *J Neurochem* 156: 16–37, 2021. doi:10.1111/jnc.15041.
23. **Geerling JC, Yokota S, Rukhadze I, Roe D, Chamberlin NL.** Kölliker-Fuse GABAergic and glutamatergic neurons project to distinct targets. *J Comp Neurol* 525: 1844–1860, 2017. doi:10.1002/cne.24164.
24. **Yokota S, Oka T, Tsumori T, Nakamura S, Yasui Y.** Glutamatergic neurons in the Kölliker-Fuse nucleus project to the rostral ventral respiratory group and phrenic nucleus: a combined retrograde tracing and in situ hybridization study in the rat. *Neurosci Res* 59: 341–346, 2007. doi:10.1016/j.neures.2007.08.004.
25. **Saunders SE, Levitt ES.** Kölliker-Fuse/parabrachial complex mu opioid receptors contribute to fentanyl-induced apnea and respiratory rate depression. *Respir Physiol Neurobiol* 275: 103388, 2020. doi:10.1016/j.resp.2020.103388.
26. **Chamberlin NL, Saper CB.** Topographic organization of respiratory responses to glutamate microstimulation of the parabrachial nucleus in the rat. *J Neurosci* 14: 6500–6510, 1994. doi:10.1523/JNEUROSCI.14-11-06500.1994.
27. **Paton JF, Dutschmann M.** Central control of upper airway resistance regulating respiratory airflow in mammals. *J Anat* 201: 319–323, 2002. doi:10.1046/j.1469-7580.2002.00101.x.
28. **Medrihan L, Tantalaki E, Aramuni G, Sargsyan V, Dudanova I, Missler M, Zhang W.** Early defects of GABAergic synapses in the brain stem of a Mecp2 mouse model of Rett syndrome. *J Neurophysiol* 99: 112–121, 2008. doi:10.1152/jn.00826.2007.
29. **Chen CY, Di Lucente J, Lin YC, Lien CC, Rogawski MA, Maezawa I, Jin LW.** Defective GABAergic neurotransmission in the nucleus tractus solitarius in Mecp2-null mice, a model of Rett syndrome. *Neurobiol Dis* 109: 25–32, 2018. doi:10.1016/j.nbd.2017.09.006.
30. **Levitt ES, Abdala AP, Paton JF, Bissonnette JM, Williams JT.** μ opioid receptor activation hyperpolarizes respiratory-controlling Kölliker-Fuse neurons and suppresses post-inspiratory drive. *J Physiol* 593: 4453–4469, 2015. doi:10.1113/JP270822.
31. **Jenkins PM, Vasavda C, Hostettler J, Davis JQ, Abdi K, Bennett V.** E-cadherin polarity is determined by a multifunction motif mediating lateral membrane retention through ankyrin-G and apical-lateral transcytosis through clathrin. *J Biol Chem* 288: 14018–14031, 2013. doi:10.1074/jbc.M113.454439.
32. **Schindelin J, Arganda-Carreras I, Frise E, Kaynig V, Longair M, Pietzsch T, Preibisch S, Rueden C, Saalfeld S, Schmid B, Tinevez JY, White DJ, Hartenstein V, Eliceiri K, Tomancak P, Cardona A.** Fiji: an open-source platform for biological-image analysis. *Nat Methods* 9: 676–682, 2012. doi:10.1038/nmeth.2019.
33. **Bosman LW, Rosahl TW, Brussaard AB.** Neonatal development of the rat visual cortex: synaptic function of GABAA receptor alpha subunits. *J Physiol* 545: 169–181, 2002. doi:10.1113/jphysiol.2002.026534.
34. **Yamada R, Kuba H.** Structural and functional plasticity at the axon initial segment. *Front Cell Neurosci* 10: 250, 2016. doi:10.3389/fncel.2016.00250.
35. **Nelson AD, Jenkins PM.** Axonal membranes and their domains: assembly and function of the axon initial segment and node of ranvier. *Front Cell Neurosci* 11: 136, 2017. doi:10.3389/fncel.2017.00136.
36. **Li W.** Excitation and inhibition imbalance in rett syndrome. *Front Neurosci* 16: 825063, 2022. doi:10.3389/fnins.2022.825063.
37. **Ezure K, Tanaka I.** GABA, in some cases together with glycine, is used as the inhibitory transmitter by pump cells in the Hering-Breuer reflex pathway of the rat. *Neuroscience* 127: 409–417, 2004. doi:10.1016/j.neuroscience.2004.05.032.
38. **Yokota S, Tsumori T, Oka T, Nakamura S, Yasui Y.** GABAergic neurons in the ventrolateral subnucleus of the nucleus tractus solitarius are in contact with Kölliker-Fuse nucleus neurons projecting to the rostral ventral respiratory group and phrenic nucleus in the rat. *Brain Res* 1228: 113–126, 2008. doi:10.1016/j.brainres.2008.06.089.
39. **Ezure K, Tanaka I, Saito Y.** Brainstem and spinal projections of augmenting expiratory neurons in the rat. *Neurosci Res* 45: 41–51, 2003. doi:10.1016/s0168-0102(02)00197-9.
40. **Yang CF, Kim EJ, Callaway EM, Feldman JL.** Monosynaptic projections to excitatory and inhibitory preBötzing complex neurons. *Front Neuroanat* 14: 58, 2020. doi:10.3389/fnana.2020.00058.
41. **Hogri R, Teuchmann HL, Heinke B, Holzinger R, Trofimova L, Sandkühler J.** GABAergic CaMKII α + amygdala output attenuates pain and modulates emotional-motivational behavior via parabrachial inhibition. *J Neurosci* 42: 5373–5388, 2022. doi:10.1523/JNEUROSCI.2067-21.2022.
42. **Wu Y, Cui N, Xing H, Zhong W, Arrowood C, Johnson CM, Jiang C.** Mecp2 disruption in rats causes reshaping in firing activity and patterns of brainstem respiratory neurons. *Neuroscience* 397: 107–115, 2019. doi:10.1016/j.neuroscience.2018.11.011.
43. **Oginsky MF, Cui N, Zhong W, Johnson CM, Jiang C.** Hyperexcitability of mesencephalic trigeminal neurons and reorganization of ion channel expression in a Rett syndrome model. *J Cell Physiol* 232: 1151–1164, 2017. doi:10.1002/jcp.25589.
44. **Kaphzan H, Buffington SA, Jung JI, Rasband MN, Klann E.** Alterations in intrinsic membrane properties and the axon initial segment in a mouse model of Angelman syndrome. *J Neurosci* 31: 17637–17648, 2011. doi:10.1523/JNEUROSCI.4162-11.2011.
45. **Shu Y, Yu Y, Yang J, McCormick DA.** Selective control of cortical axonal spikes by a slowly inactivating K+ current. *Proc Natl Acad Sci USA* 104: 11453–11458, 2007. doi:10.1073/pnas.0702041104.
46. **Maletz SN, Reid BT, Baekey DM, Whitaker-Fornek JR, Bateman JT, Bissonnette JM, Levitt ES.** Effect of positive allosteric modulation and orthosteric agonism of dopamine D2 receptors on respiration in mouse models of Rett syndrome (Preprint). *BioRxiv*, 2022. doi:10.1101/2022.04.13.488220.
47. **Julu PO, Kerr AM, Apartopoulos F, Al-Rawas S, Engerström IW, Engerström L, Jamal GA, Hansen S.** Characterisation of breathing

- and associated central autonomic dysfunction in the Rett disorder. *Arch Dis Child* 85: 29–37, 2001. doi:[10.1136/adc.85.1.29](https://doi.org/10.1136/adc.85.1.29).
48. **Mackay J, Downs J, Wong K, Heyworth J, Epstein A, Leonard H.** Autonomic breathing abnormalities in Rett syndrome: caregiver perspectives in an international database study. *J Neurodev Disord* 9: 15, 2017. doi:[10.1186/s11689-017-9196-7](https://doi.org/10.1186/s11689-017-9196-7).
49. **Bissonnette JM, Schaevitz LR, Knopp SJ, Zhou Z.** Respiratory phenotypes are distinctly affected in mice with common Rett syndrome mutations MeCP2 T158A and R168X. *Neuroscience* 267: 166–176, 2014. doi:[10.1016/j.neuroscience.2014.02.043](https://doi.org/10.1016/j.neuroscience.2014.02.043).
50. **Rozycka A, Liguz-Leczna M.** The space where aging acts: focus on the GABAergic synapse. *Aging Cell* 16: 634–643, 2017. doi:[10.1111/acer.12605](https://doi.org/10.1111/acer.12605).
51. **Gantz SC, Ford CP, Neve KA, Williams JT.** Loss of Mecp2 in substantia nigra dopamine neurons compromises the nigrostriatal pathway. *J Neurosci* 31: 12629–12637, 2011. doi:[10.1523/JNEUROSCI.0684-11.2011](https://doi.org/10.1523/JNEUROSCI.0684-11.2011).